NASA TECHNICAL MEMORANDUM

NASA TM X-71646

NASA TM X-71646

DIRECT THRUST MEASUREMENT OF A 30-CM ION THRUSTER

Bruce Banks, Vince Rawlin, Albert Weigand and John Walker
Lewis Research Center
Cleveland, Ohio 44135

TECHNICAL PAPER to be presented at
Eleventh Electric Propulsion Conference sponsored
by the American Institute of Aeronautics and Astronautics
New Orleans, Louisiana, March 19-21, 1975

DIRECT THRUST MEASUREMENT OF A 30-CM ION THRUSTER

Bruce Banks, Vince Rawlin,
Albert Weigand and John Walker
National Aeronautics and Space Administration
Lewis Research Center
Cleveland, Ohio

Abstract

A direct thrust measurement of a 30-cm diameter ion thruster was accomplished by means of a laser interferometer thrust stand. The thruster was supported in a pendulum manner by three 3.65-m long wires. Electrical power was provided by means of 18 mercury filled pots. A movable 23-button planar probe rake was used to determine thrust loss due to ion beam divergence. Values of thrust, thrust loss due to ion beam divergence, and thrust loss due to multiple ionization were measured for ion beam currents ranging from 0.5 A to 2.5 A. Measured thrust values indicate an accuracy of approximately 1% and are in good agreement with thrust values calculated by indirect measurements.

E-8215

I. Introduction

Direct thrust measurements of mercury ion thrusters can provide useful information to both electric propulsion system developers and mission planners. Recently, thrust values have been calculated using secondary measurements to correct ideal thrust for losses due to double ionization and ion beam divergence.[1][2] A direct thrust measurement allows confirmation of thrust values calculated by secondary measurements. The effects upon thrust of small changes in thruster operating conditions can be readily obtained by direct thrust measurements. Through the use of simultaneous direct thrust and ion beam probe measurements inferred values of the more difficult to obtain thrust loss due to multiple ionization can be easily calculated.

This paper describes a direct thrust measurement system which uses a laser interferometer to measure the deflection of a simple pendulum supporting a 30-cm diameter mercury ion thruster.[3][4]

II. Apparatus

Thrust Stand

A sketch of the laser interferometer thrust measurement system is shown in Figure 1. A photograph of the thrust stand is shown in Figure 2. The 30-cm diameter mercury ion thruster was suspended by three 3.65-m long wires. Electrical power was provided to the thruster by means of 18 mercury filled pots. A section view of a typical pot is shown in Figure 3. The electrical conductor rods were immersed in the mercury prior to covering the surface with approximately a 2 mm thick layer of hydrocarbon diffusion pump oil. Covering the mercury surface in this manner minimized contact resistance between the central conductor and the mercury while preventing exposure of the high vapor pressure mercury to the vacuum. The large, 7.6-cm, diameter of the mercury filled pots was chosen to reduce the possibility of transverse forces on the central conductor caused by surface menisci. Electrical strip heaters were mounted on the aluminum frame that supported the mercury filled pots. Use of these heaters in conjunction with thermocouple data from one of the pots allowed control of the mercury pot temperatures between 16.5 and 37°C for the duration of the test. In addition to providing restoring force free electrical leads to the thruster, the mercury-filled pots provided damping for pendulum oscillations.

Electron backstreaming to surfaces at a high positive potential was prevented by overlapped grounded shields over the entire thrust stand. Figure 4 is a photograph of the thrust stand with its ground shield attached in its final configuration prior to the thrust measurement. The swinging portion of the thrust stand ground shield overlapped the fixed portion for a distance of approximately 25-cm. The gap between the moving and fixed portion of the shielding was approximately 5-cm to insure that the limit of movement of the swinging portion was determined by the central conductors within the mercury-filled pots. This also established an adequate clearance for oscillation amplitude. The laser beam entered the swinging portion of the stand through a 59-cm long, 7.6-cm diameter, grounded stainless steel tube. Detection of electron backstreaming was attempted by means of a square metal plate measuring 15-cm on each side. The plate was located between the thruster and propellant tank (see Fig. 2) and was capable of being raised to the thruster high positive potential while monitoring intercepted current to it.

The laser interferometer used to measure the displacement of the moving portion of the thrust stand differed from a Michelson interferometer in that two light frequencies were used to detect relative motion.[5] The laser interferometer was a commercial unit used for precision metrology. It consists of four elements; a laser head, a remote interferometer, a corner cube, and the digital electronics. A block diagram of the interferometer is shown in Figure 5. The laser produces a 6328 Å (632.8 nm) wavelength continuous red beam which is split by Zeeman effect into two frequencies, f_1 and f_2, differing by approximately 2 MHz. Relative movement of the fixed remote interferometer (see Fig. 5) and the corner cube attached to the moving portion of the thrust stand is detected by a Doppler shift, Δf, of the heterodyne frequency $f_2 - f_1$. A distinct advantage of two frequency interferometers over a single frequency Michelson interferometer is that Fringe counting is performed on a basis of frequency variation rather than light intensity changes. As a result, attenuation resulting in up to a 95% loss of laser beam intensity due to misalignment of the laser beam has no effect upon the accuracy of the measurement. Thus the distance of approximately 4-m between the laser head and the remote interferometer had no effect upon the measurement (Fig. 5). The computer within the laser display unit was capable of digitally averaging the signal so as to reduce readout variations induced by facility vibrations. The resolution of the laser

interferometer was 2 x 10^{-6} cm however, the low frequency ($\approx$ 0.3 Hz) oscillation of the thrust pendulum limited the readable resolution to 2.5 x 10^{-4} cm.

A photograph of the laser head and display unit mounted at the top of the vacuum facility is shown in Figure 6. Initial vertical alignment of the laser beam was made prior to minor alignment adjustments made by means of turnbuckles attached to the laser head frame. Visibility of the remote interferometer from the laser head vacuum facility window to perform optical alignment was assured by installing a pilot lamp within a few centimeters of the remote interferometer.

To assure that the interferometer was properly measuring thrust pendulum deflections, a secondary pendulum movement device was also installed. This consisted of a mild steel plate mounted on the moving portion of the thrust stand that could be attracted by a solenoid electromagnet mounted on the fixed portion of the stand. The solenoid had no ferromagnetic core thus preventing the possibility of residual magnetic forces from acting upon the mild steel plate during the thrust measurement.

Thruster and Propellant Feed System

The 30-cm diameter thruster used for the test was basically a Hughes Research Laboratory 400 series thruster.[3] Major modifications were the addition of compensated dished grids, a slightly stronger main magnetic field and a shortened cathode to baffle spacing. The test thruster was operationally similar to the Hughes Research Laboratory 700 series thruster shown in cutaway view in Figure 7.[4] The geometry of the 0.4 percent compensated dished grid system used is given in Table I.

A SERT II propellant expulsion system was used to provide mercury propellant to the neutralizer, main cathode, and main vaporizer.[6] The mercury ion thruster employed electrical propellant isolators which were required to utilize a common propellant tank. The thruster and propellant tank were mounted between two 2.54-cm thick fiberglass-resin slabs, which were carefully leveled. The thruster grid system was carefully adjusted such that the centerline of the grid system was horizontal and both axisymmetric and perpendicular to one side of an imaginary triangle formed by the three thrust stand suspension wires. The neutralizer was located at the top of the thruster.

Ion Beam Divergence Measurements

A 23-button movable planar probe rake was located 2.5-m downstream of the thruster to measure ion beam divergence simultaneously with the thrust measurement. Alignment measurements were made to determine where the thruster centerline passed through the probe rake plane.

III. Evaluation of Thrust and Thrust Factors

An idealized sketch of the thrust stand pendulum is shown in Figure 8. The thrust, F, is related to the pendulum mass, M, displacement, x, pendulum length, L, and the acceleration of gravity, g, by

$$F = \frac{x\,Mg}{\sqrt{L^2 - x^2}}$$

For small x/L a simplifying approximation can be made such that

$$F = \frac{x\,Mg}{L}$$

For this thrust pendulum, $x/L \approx 2 \times 10^{-4}$, which results in 2 x 10^{-6} percent error as a result of the approximation. This is several orders of magnitude smaller than the experimentally observed standard deviation.

The three wire suspension system for the thrust pendulum assures that the thrust vector direction is independent of the displacement, x, and that the moment of inertia of the pendulum will have no effect upon its period of oscillation T.

The differential equation of motion for a damped harmonic oscillator is used to evaluate g/L in the thrust equation

$$M\ddot{x} = -\frac{Mg}{L}x - b\dot{x}$$

where
$\ddot{x}$ = acceleration
$\dot{x}$ = velocity
b = velocity damping coefficient

The resulting equation of motion is

$$x = x_0 e^{-\frac{bt}{2M}} \cos\left\{\sqrt{\frac{g}{L} - \frac{b^2}{4M^2}}\,t\right\}$$

The period of oscillation, T, for the damped harmonic oscillator is

$$T = \frac{2\pi}{\sqrt{\frac{g}{L} - \frac{b^2}{4M^2}}}$$

The value of the damping term, $b^2/4M^2$, in the period of oscillation can be determined by two measurements of oscillation amplitude at two different times. Experimental measurements taken during the thrust measurement indicated that

$$\frac{b^2}{4M^2} = 8.17 \times 10^{-5}\ \text{sec}^{-2}$$

and that

$$\frac{g}{L} = 2.69\ \text{sec}^{-2}$$

Since

$$\frac{g}{L} >> \frac{b^2}{4M^2}$$

the damped period of oscillation is very nearly equal to undamped period of oscillation. The use of the approximation that

$$\frac{g}{L} = \left(\frac{2\pi}{T}\right)^2$$

allows the thrust F to be calculated by

$$F = xM\left(\frac{2\pi}{T}\right)^2$$

The error in calculated thrust resulting from using the measured damped period of oscillation rather than the ideal undamped period of oscillation is only 0.003%.

Values for measured thrust, calculated from the previous equation, required only measurement of the pendulum displacement, pendulum mass, and the period of oscillation, T. Two corrective terms were added to the thrust calculation equation to improve the accuracy of the result. The mass of the pendulum during the thrust measurement was effectively reduced by the buoyancy of the 18 central conductor rods in their mercury pots. Also the mass of mercury in the propellant tank decreased with thruster operating time, contributing to a changing pendulum mass. The resulting equation used for the thrust measurement calculations was

$$F = x\left(M_F + \int_t^{t_0} \dot{M}dt - 18\pi\rho r^2 h\right)\left(\frac{2\pi}{T}\right)^2$$

where

M_F = final thrust pendulum mass at conclusion of direct thrust measurement

$\dot{M}$ = total mercury propellant mass flow rate at any specific time

t = time elapsed since the inception of propellant mass flow

t_0 = time elapsed from beginning to end of propellant mass flow

ρ = density of mercury in the mercury-filled pots, 13.546 gms/cm^3

r = radius of the central conductors in the mercury-filled pots

h = depth of immersion of the central conductors in the mercury-filled pots

The thrust, F, as expressed by the previous equation is the thrust measured in the direction of anticipated thrusting. The magnitude of the actual thrust vector would be larger by $1/\cos\phi$ where ϕ is the thrust misalignment angle. The movable planer probe rake was used to determine ϕ.

A measured total thrust factor, f_T, was calculated by

$$f_T = \frac{F}{F_I}$$

Where F is the measured thrust and F_I is the ideal thrust assuming the beam is comprised only of paraxial directed singly charged mercury ions. Thus

$$F_I = J_B\sqrt{\frac{2m\ V_{NET}}{e}}$$

where

m = mercury ion mass = 3.33085×10^{-25} kg

e = electron charge = 1.60219×10^{-19} C

J_B = ion beam current, A

V_{NET} = net accelerating potential, v

F_I = ideal thrust, N

or

$$F_I \cong (2.03909 \times 10^{-3})\ J_B\sqrt{V_{NET}}$$

A measured ion beam divergence factor, f_D, was calculated from the 23-button probe rake data assuming an ion beam point source. Thus

$$f_D = \frac{\sum_{i=1}^{23} J_{P_i} R_i \cos\theta_i}{\sum_{i=1}^{23} J_{P_i} R_i}$$

where

J_{P_i} = probe current for the i^{th} probe

R_i = distance from the i^{th} probe to the centerline of the ion beam

θ_i = angle formed by intersection of a line extending from the center of the thruster grid system to the i^{th} probe and the centerline of the ion beam.

The above formula assumes that the ion beam profile has circular symmetry.

The thrust loss due to multiple charged ions in the beam was calculated indirectly as an inferred multiple ion thrust factor, F_M, where

$$f_M = \frac{f_T}{f_D}$$

Thus the measured thrust, F, is given by

$$F = f_D f_M F_I$$

IV. Procedure

Measurements were taken to determine the total amount of propellant consumed during the thrust

measurment by obtaining propellant tankage masses before and after the test. This allowed a more accurate estimate of the term

$$\int_t^{t_0} \dot{M} dt$$

The depth of immersion, h, of the central conductors in the mercury-filled pots was measured while the thrust stand was assembled but not at vacuum. Initially there was a concern that the immersion depth might change upon evacuation of the 7.6-m diameter vacuum facility. Measurements made to determine the amount of vacuum facility distortion indicated that the immersion depth change would be less than 0.1 mm, resulting in less than a 10^{-3} percent error in the thrust value.

The period of oscillation, T, was measured in vacuum with the mercury filled pots both at the beginning and end of the thrust measurement test. The electromagnet was cycled to increase the pendulum oscillation amplitude until at least 40 pendulum oscillations could be counted on the interferometer readout before the oscillations damped out. During the 14 hour thrust measurement period, the general sequence of thruster operating conditions for each thrust measurement consisted of:

1) thruster off
2) thruster operating at standard condition
3) thruster operating with some variation from the standard condition
4) thruster operating at standard condition

.
.
.

n) thruster off
n+1) thruster operating at a new standard condition

.
.
.

The placement of thruster-off and thruster operating-at-a standard-condition tests in sequence was for purposes of obtaining absolute thrust values. The insertion of a thruster operating condition with some variation from the standard condition between two standard conditions permitted the detection of small changes in thrust caused by alterations in operating parameters. Ion beam current density profile data was taken via the 23-button planar probe rake for most of the pertinent thruster operating conditions.

At the conclusion of the thrust measurement test the total thrust pendulum mass and the residual mercury propellant mass was measured and documented.

V. Results and Discussion

Thrust Measurements

One of the most significant result of the direct thrust measurement is that the thrust measurement system successfully functioned as planned during the first test, allowing all the thrust measurements to be taken on a single day during one 14 hour period. This is a manifestation of the simplicity of the pendulum thrust stand which does not require a thrust calibration, combined with the inherent accuracy of the laser interferometer.

The resulting parameters required to calculate thrust are shown in Table II. The values of

$$\int_t^{t_0} \dot{M} dt, \; x, \text{ and } F,$$

of course, depend upon time and the particular thruster operating condition. For purposes of completing Table II, values listed are those typical of the thruster operating at the standard condition shown in Table III. The measured thrust value shown in Table II is the average value of 10 thrust measurements taken at different times with the thruster operating as described in Table III.

The misalignment of the thrust vector with respect to the intended thrusting direction, documented by means of the movable ion beam probe rake, indicated a 0.9° misalignment. This would result in only a 0.01% thrust loss.

A plot of the probe rake data showing contours of constant current density is shown in Figure 9. The plotting technique used was similar to that employed in reference 7. The contour plot appears to have circular symmetry with a slight eliptical distortion except at the outermost low current density contour where a hexagonal distortion is apparent. It is possible that the distortion is caused by a slight hexagonal beamlet structure due to the hexagonal array of holes. Experimental evidence of hexagonal beamlet structure is given in references 8 and 9. The grid system hole array was oriented so that the rows of holes were aligned along the vertical axis. The orientation of the superposed hexagonal beamlets is consistant with the observed ion beam profile orientation. The outermost grid holes are probably the most significant contributor to the slight hexagonal ion beam profile envelope.[9] This could be due to ion extraction sheath distortion caused by near adjacent holes whose sheaths are also protruding into the discharge chamber because of the low current density of the beamlets.

Measurements of the ion beam divergence thrust factor, computed by traversing the beam with the probe rake, were in agreement with values calculated from a stationary rake assuming circular symmetry of the ion beam.

Values of measured thrust, measured total thrust factor, measured beam divergence thrust factor, and inferred multiple ion thrust factor are presented in Tables IV through VIII for ion beam currents from 0.5 A to 2.5 A.

The values for the ion beam divergence thrust factors are approximately 1% lower than those in reference 2 and 2% higher than those in reference 7. Known differences in dish depth, compensation, dishing technique, grid thickness, grid hole diameter and point or distributed source assumptions could

easily explain the observed divergence thrust factor dissimilarities.

Thrust loss due to multiple ionization was predominantly due to doubly charged ions. Triply charged ions have been detected, but represent less than one tenth of the double ion density.[2] The inferred multiple ion thrust factor for the standard operating condition in Table VII is approximately 1% lower than measured values for the thruster in reference 5 operated at the same discharge voltage but 10 A emission current. Figure 10 indicates the magnitude of the inferred multiple ion thrust factor as a function of discharge voltage for two ion beam currents (the data is taken from Tables VI and VII).

The dependence of the divergence, multiple ion and total thrust factors upon ion beam current is illustrated in Figure 11. The divergence thrust factor increases with beam current, while the multiple ion thrust factor decreases with increasing beam current. The product of these two parameters is equal to the total thrust factor which is near maximum over a broad range from 0.5 A to 2.0 A beam current. The datum point for the multiple ion thrust factor at 1.0 A beam current is anomalously low.

Operation of the thruster at various ion beam currents results in different magnitude current loops. The largest area current loop is probably the ion beam neutralization current loop. Its magnetic dipole would tend to cause torques upon the thrust pendulum if the earths magnetic field is of sufficient magnitude and proper orientation within the vacuum facility. However, no changes in the pointing direction of the thruster were observed for beam currents from 0.5 A to 2.5 A, indicating that these torques had a neglible effect upon the thrust measurements.

The neutralizer discharge should contribute less than 10^{-4} N to measured thrust and as such have no effect upon the measured values.[10]

Operation of the thruster using vacuum facility neutralization as shown in Table VII has very little effect upon the measured thrust. An 8 volt increase in the plasma potential downstream of the thruster, for the facility neutralized condition, would account for the small discrepancy between this operating condition and the standard condition.

Error Analysis

The estimated probable errors of the parameters used to calculate thrust for the standard thruster operating condition are listed in Table II. The estimated probable errors were calculated from the equation

$$F = x\,(M_F + M_T - 18\pi\rho r^2 h)\left(\frac{2\pi}{T}\right)^2$$

where

$$M_T \int_t^{t_0} \dot{M}dt$$

The estimated probable error in F is given by

$$P_F = \left[\sum_i \left(\frac{\partial F}{\partial i}\right)^2 P_i^2\right]^{1/2}$$

where $i = x, M_F, M_T, \rho, r, h,$ and T and P_i is the estimated probable error in the measurement of the i^{th} variable. Values from Table II were then substituted in the above equation to yield

$$P_F = 0.00083\ N = 0.65\%\ of\ F$$

The percentage contribution of the various parameters to the probable error of the measured thrust is simply

$$\frac{\left(\frac{\partial F}{\partial i}\right)^2 P_i^2}{P_F^2}(100\%) = \frac{\left|\frac{\partial F}{\partial i}\right| P_i}{P_F}(100\%)$$

As shown in Table II, the pendulum displacement, x, and its period of oscillation, T, share almost equally in accounting for 97.5% of the estimated probable error in the measured thrust.

The preceeding error analysis represents a measure of the absolute accuracy of thrust measurement. The sensitivity of the thrust stand to variations in thrust that do not require a complete set of measurements to be made, would be detectable to a finer degree. Only x and

$$M_T = \int_t^{t_0} \dot{M}dt$$

were determined for each measurement of F. Thus variations in thrust should be capable of being detected down to approximately 0.0004 N even though the estimated probable absolute error of the measurement is twice that value. Similarly because only x and M_T were determined for each measurement, an observed standard deviation would be smaller than predicted by an estimated standard deviation in which all parameters were measured for each datum point. There is an uncertainty in the actual thrust because it is determined by meter readings that have their own inherent uncertainties. The estimated standard deviation in measured thrust, σ_F, should reflect the data taking technique and the thrust setting inaccuracies.

The calculation of these combined deviations shall be accomplished by first evaluating the estimated probable error in thrust caused by meter reading inaccuracy, then combining this result with the pertinent thrust measurement technique probable errors.

The estimated probable error in actual thrust due to thruster meter reading inaccuracy is given by

$$P_{\mathcal{F}} = \left[\sum_i \left(\frac{\partial \mathcal{F}}{\partial i}\right)^2 P_i^2\right]^{1/2}$$

where

$i = f_D, f_M, J_B, V_{NET}$

$\mathcal{F} \cong f_D f_M (2.03909 \times 10^{-3}) J_B \sqrt{V_{NET}}$

Here f_D and f_M are the actual thrust factors for ion beam divergence and multiple ionization (in distinction to the measured thrust factors f_D and f_M). If the estimated fractional probable errors in f_D and f_M are much less than those for J_B and V_{NET} then

$$P_{\mathcal{F}} \cong \mathcal{F} \left[\left(\frac{P_{J_B}}{J_B} \right)^2 + \left(\frac{1}{2} \frac{P_{V_{NET}}}{V_{NET}} \right)^2 \right]^{1/2}$$

Using the standard condition values with

$$P_{J_B} = 0.01 \text{ A and } P_{V_{NET}} = 10 \text{ V}$$

results in

$$P_{\mathcal{F}} \cong 0.00085 \text{ N} = 0.67\% \text{ of } \mathcal{F}.$$

It is fortuitous that the estimated probable error of the thrust measuring device (0.65% of the measured thrust) is approximately equal to the estimated probable error in actual thrust due to thruster meter reading inaccuracy.

The combined effect of thrust measuring and thrust setting techniques should result in an estimated standard deviation, σ_F, given by

$$\sigma_F = \left[\left(\frac{\partial F}{\partial x} \right)^2 \sigma_x^2 + \left(\frac{\partial F}{\partial M_T} \right)^2 \sigma_{M_T}^2 + \sigma_{\mathcal{F}}^2 \right]^{1/2}$$

where for normally distributed data

$$\sigma_i \cong 1.48 \, P_i$$

where

$i = x, M_T$, and F

For the standard operating condition, the estimated standard deviation in measured thrust results in

$$\sigma_F = 0.0015 \text{ N} = 1.2\% \text{ of F}$$

The actual observed standard deviation for 10 standard condition thrust measurements is 0.0012 N or 0.9% of the measured thrust F.

Considering the very small statistical sample size there appears to be reasonable agreement between predicted and actually measured standard deviation.

VI. Conclusions

A laser interferometer thrust stand has been developed that measures the actual thrust of a 30-cm diameter thruster. The resulting thrust values are typically accurate to within 1% based upon both a probable error analysis and statistical test results. The inherent simplicity of the thrust pendulum allows numerous measurements to be taken in a short amount of time thus providing information concerning small thrust changes from variations in thruster operating conditions. The resulting data also confirms the reliability of indirect thrust measurement techniques. The precision of the thrust measuring device appears to be equal to the precision to which the actual thrust could be set using its power supply meters.

References

1. Vahrenkamp, R. P., "Measurement of Double Charged Ions in the Beam of a 30-cm Mercury Bombardment Thruster," AIAA Paper 73-1057, Lake Tahoe, Nev., 1973.
2. Poeschel, R. L., "A 2.5 kW Advanced Technology Ion Thruster," Hughes Research Labs., Malibu, Calif., 1974; available as CR-134687, NASA.
3. Rawlin, V. K., "Performance of 30-cm Ion Thruster with Dished Accelerator Grids," AIAA Paper 73-1053, Lake Tahoe, Nev., 1973.
4. Poeschel, R. L., King H. J., and Schnelker, D. E. "An Engineering Model 30-cm Ion Thruster," AIAA Paper 73-1084, Lake Tahoe, Nev., 1973.
5. Dukes, John N. and Gordon, Gary B., "A Two-Hundred-Foot Yardstick with Gradations Every Microinch," Hewlitt-Packard Journal, Vol. 21, No. 12, Aug. 1970.
6. Kerslake, W. R., Goldman, R. G., and Nieberding, W. C., "SERT II - Mission, Thruster Performance, and in-Flight Measurements," Journal of Spacecraft and Rockets, Vol. 8, No. 3, Mar. 1971, pp. 213-224.
7. Danilowicz, R. L., Rawlin, V. K., Banks, B. A., and Wintucky, E. G., "Measurement of Beam Divergence of 30-Centimeter Dished Grids," AIAA Paper 73-1051, Lake Tahoe, Nev., 1973.
8. Byers, D. C. and Banks B. A., "Beam Focusing Characteristics of Variously Shaped Grid Holes," TMX-67922, Sept. 1971, NASA.
9. "8-cm Mercury Ion Thruster System Technology," AIAA Paper 74-1116, San Diego, Calif., 1974.
10. Snyder, A., and Banks, B. A., "Thrust Measurements of a Hollow-Cathode Discharge," TND-6705, March 1972, NASA.

Table 1 Grid geometry

	Screen grid	Accelerator grid
Hole dia, mm	1.91	1.52
Hole array, center-to-center spacing, mm	(2.?1)(0.996)	2.21
Thickness, mm	0.38	0.51
Percent open area	67	43
Cold grid to grid spacing, mm		0.6 - 0.8
Active diameter, cm		28.6
Dish depth, cm		2.29
Dish radius of curvature, cm		51.9
Diameter of dished region, cm		30.48
Dish direction:		Ion flow

Table II Values of thrust measurement parameters

Parameter	Symbol	Unit	Value	Estimated probable error, P_i	Percentage contribution to estimated probable error of measured thrust, %
Final thrust pendulum mass	M_F	kg	86.349	0.023	0.17
Propellant mass consumed during the remainder (t_0 - t sec) of the test	$\int_t^{t_0} \dot{M} dt$	kg	0.055*	3.0×10^{-3}*	0.003
Density of mercury in mercury filled pots	ρ	kg/m^3	1.3546×10^{4}	4.2×10^{-3}	1×10^{-12}
Radius of central conductors in mercury-filled pots	r	m	3.175×10^{-3}	6.4×10^{-4}	2.0
Depth of immersion of central conductors in the mercury-filled pots	h	m	2.54×10^{-2}	3.8×10^{-3}	0.27
Period of oscillation of thrust pendulum	T	sec	3.80825	0.0085	47.1
Thrust pendulum displacement	x	m	5.416×10^{-4}*	2.5×10^{-6}*	50.4
Measured thrust	F	N	0.1271*	0.00083*	100

*Parameter varies widely through test depending on time and thruster operating conditions. A typical (see Table III) value is listed simply to show relative magnitudes.

Table III Standard thruster operating conditions

Ion beam current, J_B	2.0 A
Net accelerating potential, V_{NET}	1137 V
Accelerator voltage, V_A	-500 V
Discharge voltage, ΔV_I	37 V
Emission current, J_E	12 A

Table IV Thrust measurement at 0.5 A ion beam current

Net accelerating potential, V_{NET}, V	Accelerator voltage V_A, V	Discharge voltage, ΔV_I, V	Emission current, J_E, A	Measured thrust, F, N	Measured total thrust factor, f_T	Measured beam divergence thrust factor, f_D	Inferred multiple ion thrust factor, f_M
1137	-500	37	3.0	0.0319	0.927	0.953	0.973

Table V Thrust measurements at 1.0 A ion beam current

Net accelerating potential, V_{NET}, V	Accelerator voltage, V_A, V	Discharge voltage, ΔV_I, V	Emission current, J_E, A	Measured thrust, F, N	Measured total thrust factor, f_T	Measured beam divergence thrust factor, f_D	Inferred multiple ion thrust factor, f_M	Description
1137	-500	37	6.0	0.0632	0.919	0.962	0.956	
1143	-500	43	6.0	0.0626	0.908	0.962	0.944	High ΔV_I

Table VI Thrust measurements at 1.5 A ion beam current

Net accelerating potential, V_{NET}, V	Accelerator voltage, V_A, V	Discharge voltage, ΔV_I, V	Emission current, J_E, A	Measured thrust, F, N	Measured total thrust factor, f_T	Measured beam divergence thrust factor, f_D	Inferred multiple ion thrust factor, f_M	Description
1137	-500	37	8.9	0.0957	0.928	0.970	0.957	
737	-500	37	8.9	0.0763	0.919	0.977	0.941	Low V_{NET}
1537	-500	37	8.9	0.1108	0.924	0.963	0.959	High V_{NET}
1137	-250	37	8.9	0.0971	0.942	0.980	0.961	Low $\|V_A\|$
1137	-900	37	8.9	0.0941	0.913	0.954	0.957	High $\|V_A\|$
1133	-500	33	8.9	0.0971	0.943	0.971	0.971	Low ΔV_I
1143	-500	43	8.9	0.0935	0.905	0.961	0.942	High ΔV_I

Table VII Thrust measurements at 2.0 A ion beam current

Net accelerating potential, V_{NET}, V	Accelerator voltage, V_A, V	Discharge voltage, ΔV_I, V	Emission current, J_E, A	Measured thrust, F, N	Measured total thrust factor, f_T	Measured beam divergence thrust factor, f_D	Inferred multiple ion thrust factor, f_M	Description
1137	-500	37	12	0.1271	0.925	0.976	0.947	Standard condition
737	-500	37	12	0.1025	0.926	0.980	0.945	Low V_{NET}
1537	-500	37	12	0.1496	0.936	0.969	0.966	High V_{NET}
1137	-250	37	12	0.1282	0.932	0.984	0.947	Low $\|V_A\|$
1137	-900	37	12	0.1258	0.918	0.961	0.955	High $\|V_A\|$
1133	-500	33	12	0.1299	0.946	0.976	0.969	Low ΔV_I
1143	-500	43	12	0.1240	0.899	0.976	0.921	High ΔV_I
1137	-500	37.3	12	0.1264	0.919	0.975	0.942	Neutralizer off with tank neutralization

Table VIII Thrust measurements at 2.5 A ion beam current

Net accelerating potential, V_{NET}, V	Accelerator voltage, V_A, V	Discharge voltage, ΔV_I, V	Emission current, J_E, A	Measured thrust, F, N	Measured total thrust factor, f_T	Measured beam divergence thrust factor, f_D	Inferred multiple thrust factor, f_M
1137	-500	37	15.0	0.1563	0.909	0.980	0.928

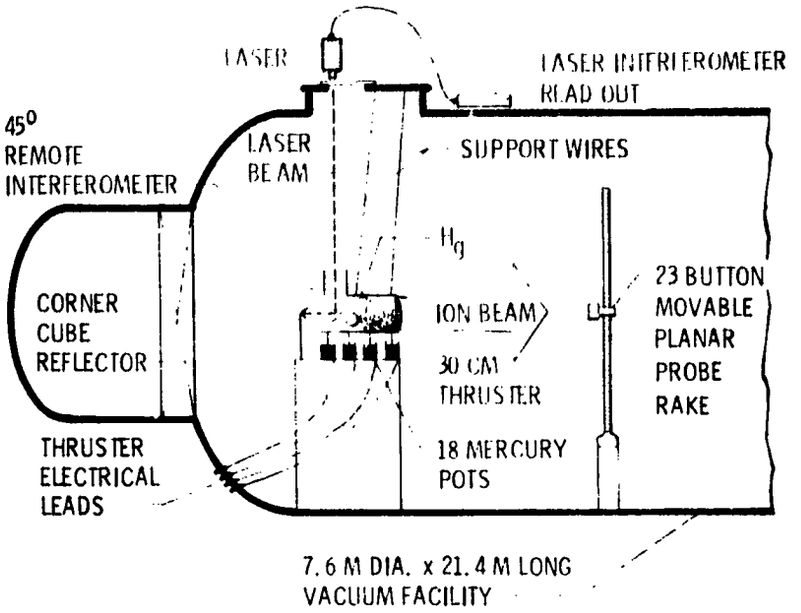

Figure 1. - Laser interferometer thrust measurement system.

E-8215

Figure 2. - Thrust stand. (Ground screen, remote interferometer and corner cube reflector are not shown.)

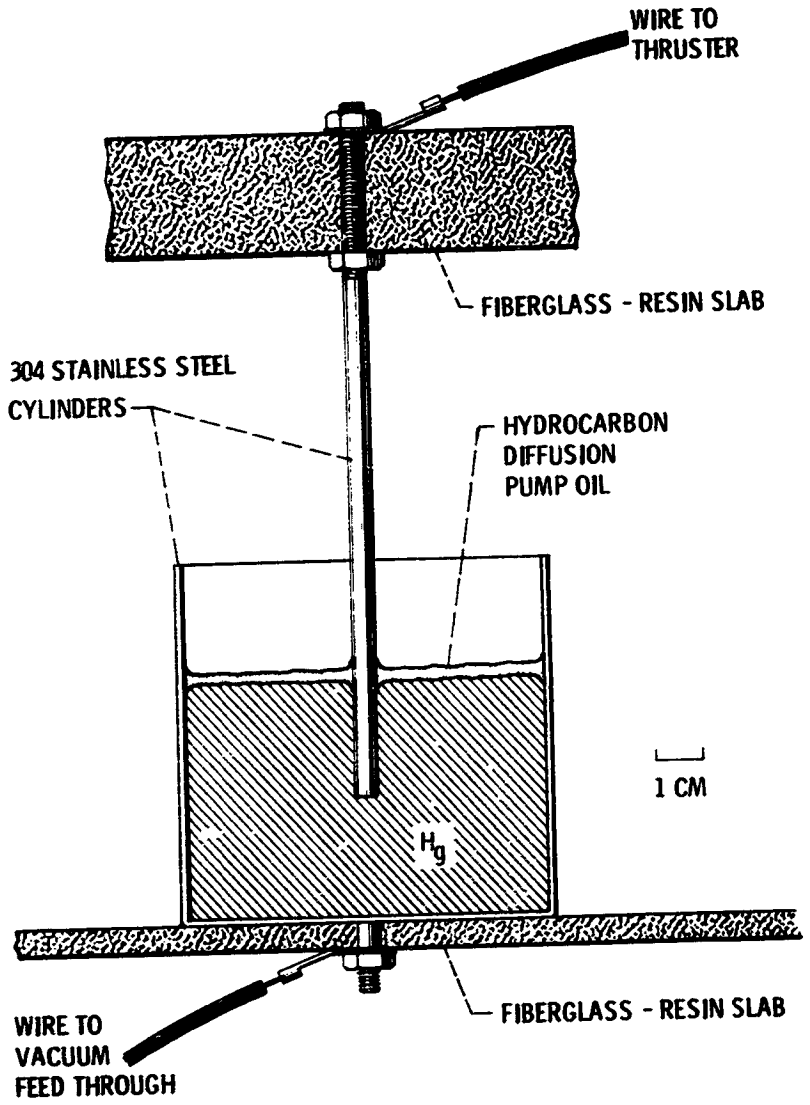

Figure 3. - Mercury filled pot.

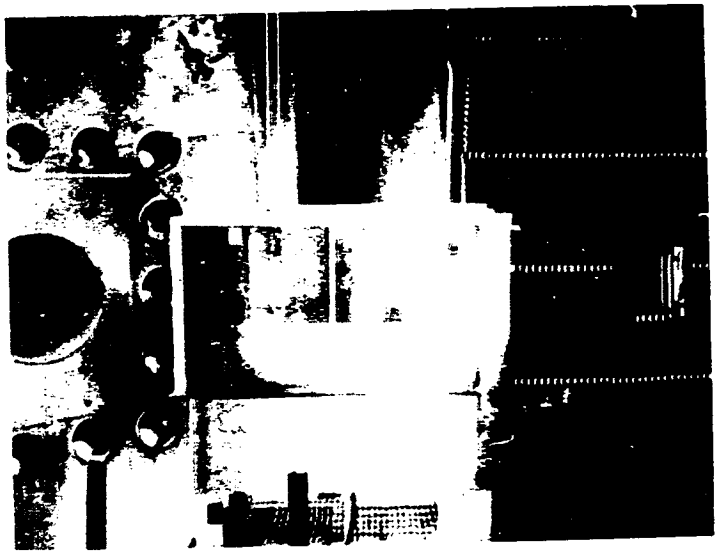

Figure 4. - Thrust stand with ground shielding attached immediately prior to thrust measurement test.

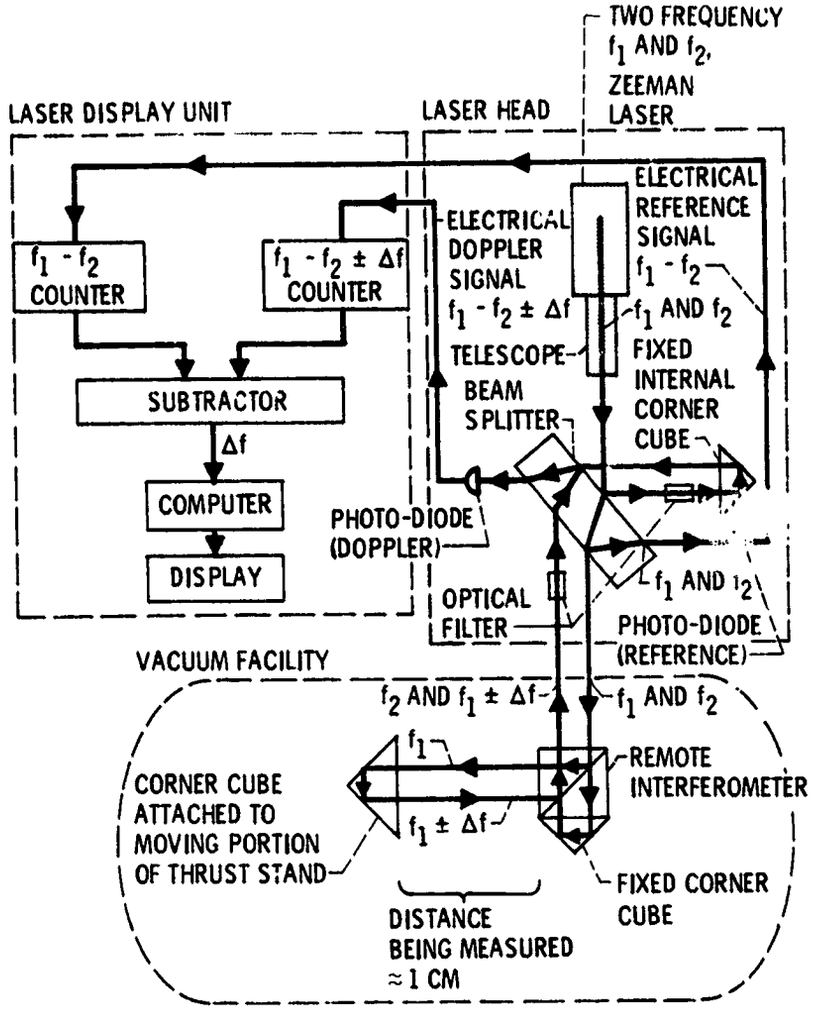

Figure 5. - Laser interferometer block diagram.

E-8215

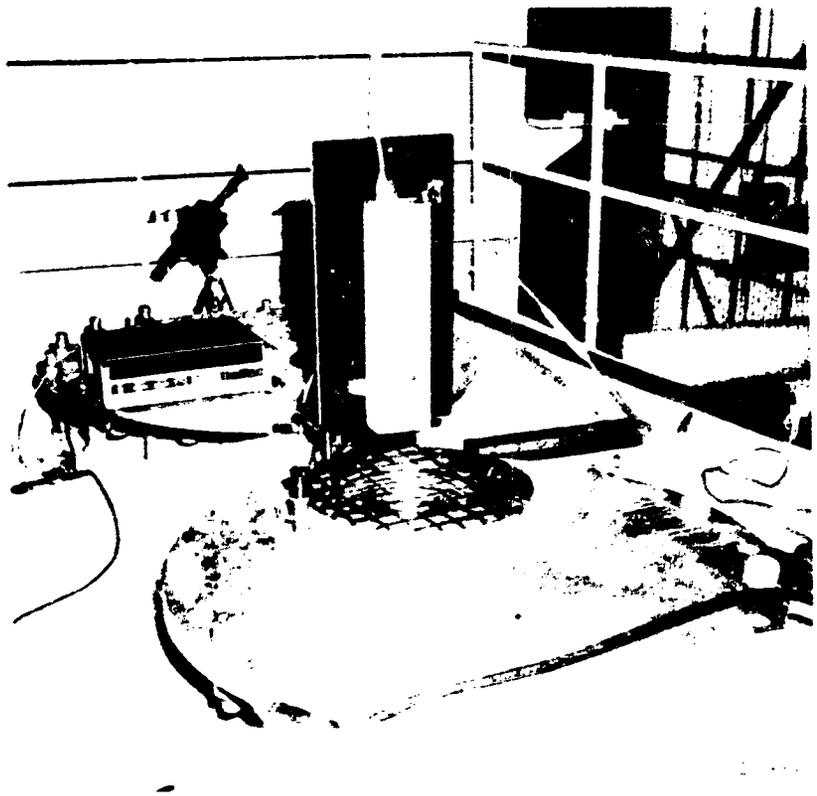

Figure 6. - Laser head and display unit at top of vacuum facility.

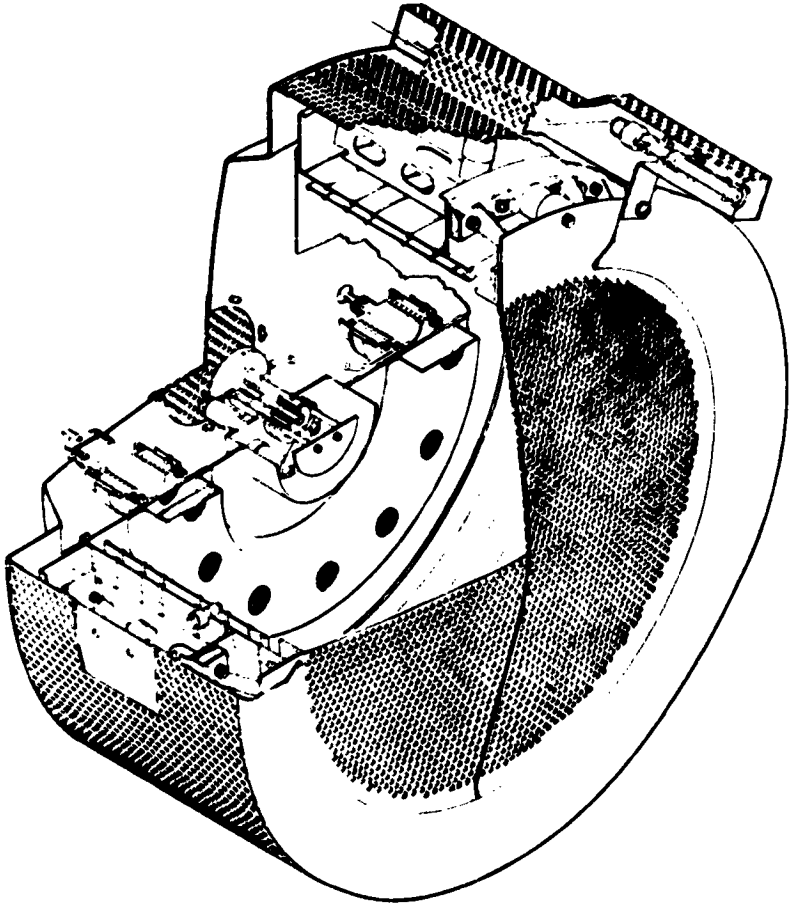

Figure 7. - 30 cm diameter mercury ion thruster.

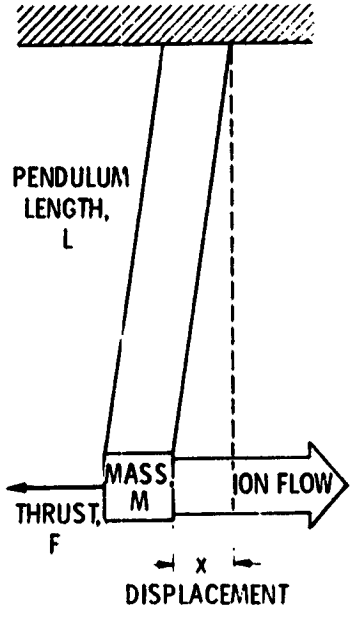

Figure 8. - Ideal thrust-stand pendulum.

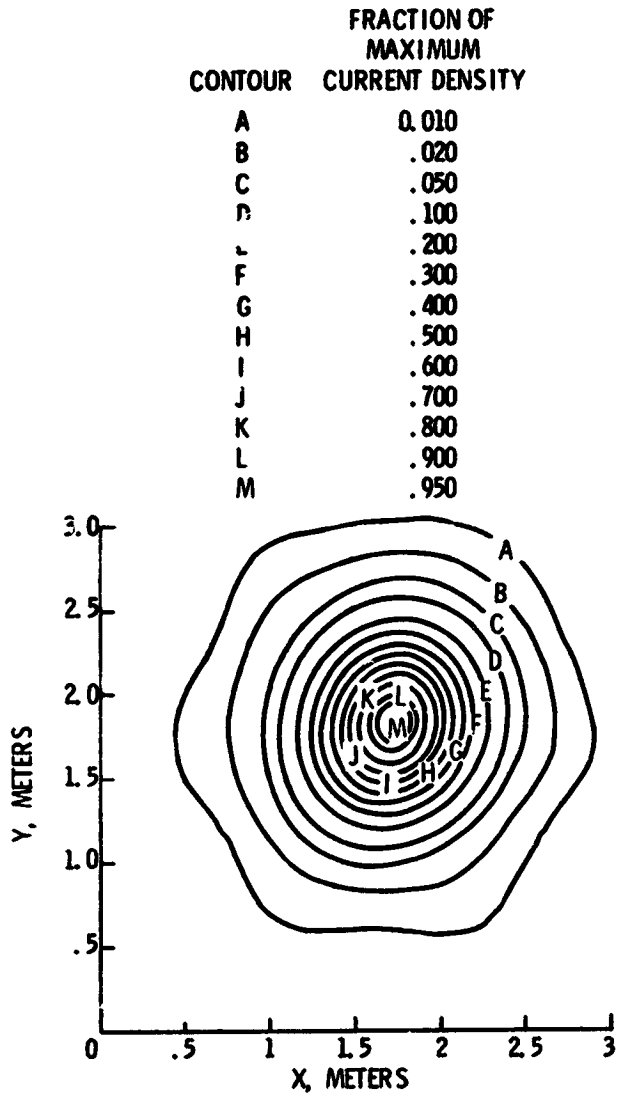

Figure 9. - Ion beam profile at standard operating conditions taken in a plane 2.5 m downstream of the thruster.

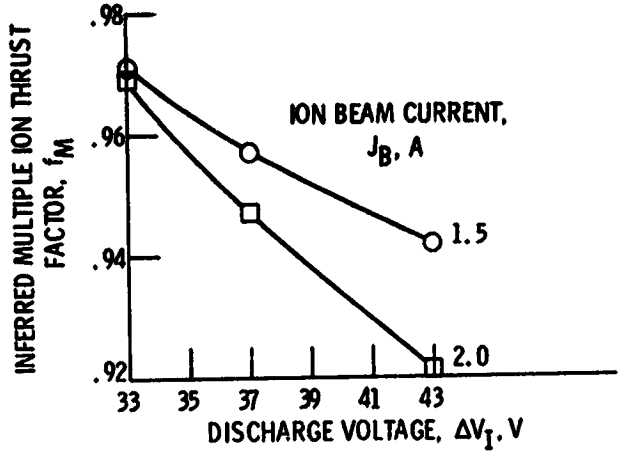

Figure 10. - Inferred multiple ion thrust factor dependence upon discharge voltage.

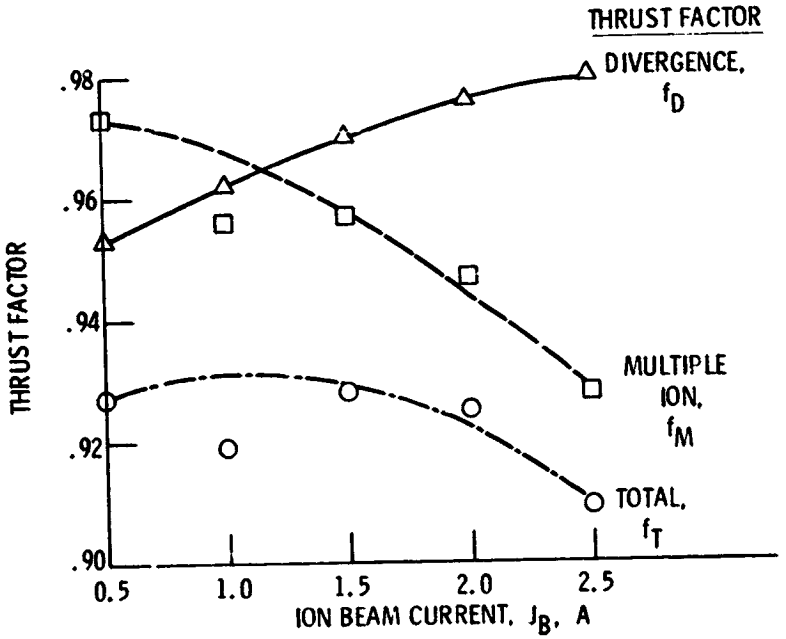

Figure 11. - Variation of thrust factors with ion beam current

E-8215

NASA-Lewis